nature communications

Article

https://doi.org/10.1038/s41467-025-59417-7

Closed-loop control of theta oscillations enhances human hippocampal network connectivity

Received: 18 April 2024

Accepted: 16 April 2025

Published online: 30 April 2025

Check for updates

James E. Kragel[1] ✉, Sarah M. Lurie[2], Naoum P. Issa[1], Hiba A. Haider[1], Shasha Wu[1], James X. Tao[1], Peter C. Warnke[3], Stephan Schuele[4], Joshua M. Rosenow[5], Christina Zelano[4], Mark Schatza[6], John F. Disterhoft[7], Alik S. Widge[6] & Joel L. Voss[1]

Theta oscillations are implicated in regulating information flow within cortico-hippocampal networks to support memory and cognition. However, causal evidence tying theta oscillations to network communication in humans is lacking. Here we report experimental findings using a closed-loop, phase-locking algorithm to apply direct electrical stimulation to neocortical nodes of the hippocampal network precisely timed to ongoing hippocampal theta rhythms in human neurosurgical patients. We show that repetitive stimulation of lateral temporal cortex synchronized to hippocampal theta increases hippocampal theta while it is delivered, suggesting theta entrainment of hippocampal neural activity. After stimulation, network connectivity is persistently increased relative to baseline, as indicated by theta-phase synchrony of hippocampus to neocortex and increased amplitudes of the hippocampal evoked response to isolated neocortical stimulation. These indicators of network connectivity are not affected by control stimulation delivered with approximately the same rhythm but without phase locking to hippocampal theta. These findings support the causal role of theta oscillations in routing neural signals across the hippocampal network and suggest phase-synchronized stimulation as a promising method to modulate theta- and hippocampal-dependent behaviors.

Theta oscillations are hallmark electrophysiological features of the rodent hippocampus[1–3] and have been associated with human hippocampus-dependent memory[4]. A prominent hypothesis of memory function proposes that the hippocampus coordinates activity[5,6] across large-scale distributed networks[7,8]. Inter-regional network communication is thought to be coordinated by theta dynamics[6,9], (although additional mechanisms of inter-regional communication are possible[10]). In rodents, experimental disruption of theta causes memory deficits[11], and hippocampal theta is disrupted by neurodegenerative disease and age in transgenic Alzheimer's disease model animals[12]. However, direct evidence linking hippocampal theta to the network communication thought to support memory in humans is lacking.

Theta-rhythmic direct electrical stimulation (DES) has been used in efforts to modulate oscillatory dynamics and rescue memory

[1]Department of Neurology, University of Chicago, Chicago, IL, USA. [2]Interdepartmental Neuroscience Program, Northwestern University, Feinberg School of Medicine, Chicago, IL, USA. [3]Department of Neurological Surgery, University of Chicago, Chicago, IL, USA. [4]Department of Neurology, Northwestern University, Feinberg School of Medicine, Chicago, IL, USA. [5]Department of Neurosurgery, Northwestern University, Feinberg School of Medicine, Chicago, IL, USA. [6]Department of Psychiatry, University of Minnesota, Minneapolis, MN, USA. [7]Department of Neuroscience, Northwestern University, Feinberg School of Medicine, Chicago, IL, USA. ✉e-mail: jkragel@uchicago.edu

function in humans[13–17]. However, because the effects of stimulation depend upon the ongoing brain state[18–23], it has proven difficult to reliably affect these targets. Within hippocampal circuits, the phase of ongoing theta rhythms is one such state that determines the outcome of stimulation. Theta phase modulates both network communication[24,25] and synaptic plasticity[1,26–28], which could mediate the effects of stimulation on memory[29]. It may thus be possible to more effectively modulate hippocampal networks by timing stimulation to the phase of ongoing theta rhythms.

However, how theta-synchronized DES affects hippocampal networks remains unclear. One possibility is that stimulation timed to theta will entrain the network at theta frequencies[30], yielding plasticity that increases theta synchrony between the hippocampus and other network locations. To test this prediction, we used closed-loop control to precisely time stimulation of the lateral temporal cortex (LTC) to hippocampal theta oscillations recorded in real time. The logic of this closed-loop implementation is that endogenous theta rhythms can be "nudged" in desired directions by appropriately timed stimulation[31], in contrast to previous approaches that attempt to impose an exogenous theta rhythm via theta-rhythmic stimulation[30]. Stimulated regions of LTC were selected based on their connectivity with hippocampus, such that stimulation would be expected to trans-synaptically influence hippocampal activity and affect network communication[32,33].

We reasoned that repetitive theta-synchronized stimulation would have both immediate and persistent effects on network function. We predicted that theta-synchronized stimulation would entrain the network, as indicated by immediate increases in hippocampal theta. We also predicted that a prolonged period of repetitive theta-synchronized stimulation would lead to plasticity in network synchrony, producing changes in network connectivity that persist beyond the period of stimulation. We tested these predictions relative to control stimulation applied to comparable locations and parameters, but that was not phase locked to hippocampal theta. We used two complementary measures of connectivity, stimulation-evoked potentials (SEPs, also referred to as cortico-cortical evoked potentials, e.g., ref. 34) and phase-alignment of spontaneous activity, to test for converging evidence for changes to the network. This experiment thus directly evaluated the role of hippocampal theta in supporting network communication thought to underlie memory in humans.

Results

Theta-synchronized DES of hippocampal networks

As is the case for stimulation of many nodes of the hippocampal network[35], DES of the LTC evokes potentials in the hippocampus[25], reflecting effective connectivity of LTC with hippocampus[36,37]. In addition, the phase of ongoing theta oscillations determines the strength of the evoked response in the hippocampus to LTC stimulation[25], indicating optimal theta phases for the propagation of signals from LTC to hippocampus. Repetitive stimulation paradigms designed to modulate network function should be more effective when stimulation is delivered in a phase-dependent manner[38,39]. We therefore developed a closed-loop paradigm to causally test whether theta oscillations control the effects of DES across hippocampal networks (Fig. 1A). We assessed changes in network physiology, including hippocampal responses to single-pulse electrical stimulation (SPES), while participants comfortably rested (Fig. 1B). We used SPES to quantify changes in direct connectivity[36,40] and excitability[41,42] within the network by measuring the amplitude of early (within 50 ms) evoked potentials following stimulation. We also examined the amplitude of later (up to 250 ms following stimulation) evoked potentials thought to reflect multi-node propagation across networks, such as seen when following signals from the hippocampus and anterior thalamus to the cingulate cortex[43]. Finally, we examined whether changes in effective connectivity were predicted by the magnitude and synchrony of theta oscillations, as predicted by the communication-through-coherence hypothesis[9,44]. This paradigm allowed us to measure immediate changes in the network during the repetitive stimulation period itself and persistent changes in the network in the minutes after repetitive stimulation (Post) by comparisons to the pre-stimulation baseline (Pre).

Theta bursts were prevalent throughout hippocampal sites in the moments leading up to our stimulation protocol (Fig. 1C), providing a real-time signal to phase synchronize stimulation[45]. We delivered a total of 3448 stimulation pulses to four participants during theta-synchronized (TS) stimulation, and 5302 stimulation pulses to five participants during phase-blind (PB) control stimulation (two participants were stimulated in both conditions). Figure 1D depicts the stimulation-locked LFP in an example participant, revealing consistent delivery at the trough of hippocampal theta in the TS but not the PB condition. TS stimulation occurred near the theta trough in each participant, as intended (Fig. 1E, Table S2). Comparing phase-locking of stimulation to hippocampal theta (Fig. 1F) revealed significantly greater phase-locking in the TS compared to the PB condition ($\bar{r}_{TS} = 0.61(\pm 0.03)$, $\bar{r}_{PB} = 0.02(\pm 0.01)$, $F(1, 2.6) = 469.6$, $p < 0.001$), as expected. This paradigm thus afforded us the opportunity to assess how repetitive theta-synchronized stimulation modulates cortico-hippocampal network activity.

Enhancement of theta oscillations and connectivity during theta-synchronized stimulation

We characterized the immediate impact of TS stimulation on hippocampal theta during the 30-minute period when TS stimulation was delivered repetitively, relative to the period of repetitive PB stimulation. Although TS stimulation was delivered far slower than the theta rhythm (at less than one pulse per second), we reasoned that TS stimulation would enhance hippocampal network theta oscillations via entrainment because of its phase synchronization to hippocampal theta[16,30]. To test this, we examined changes in hippocampal theta over the course of the TS or PB repetitive stimulation periods. We separated stimulation-evoked activity from endogenous oscillatory activity using generalized eigenvalue decomposition[46,47] (see Methods and Fig. S4). This approach led to the removal of stimulation-evoked activity, as evident by reduced SEP peak-to-peak amplitude ($F(1, 5.26) = 5.3$, $p = 0.03$). A related caveat is that this approach will remove stimulation-locked theta oscillations (see Fig. S4C for examples). Remaining theta bouts observed in the inter-stimulus interval must occur at random times relative to stimulation. As such, these analyses may underestimate the overall effects of stimulation on theta. After removing sources related to stimulation artifact and stimulus-locked neural responses, we asked whether theta power and synchrony (measured using the phase lag index (PLI)[48]) increased throughout the repetitive stimulation period. We also asked whether changes in network plasticity occurred over the course of repetitive stimulation, measured by changes in SEP magnitude with additional stimulation pulses.

Figure 2A shows correlations between hippocampal power and time within the repetitive stimulation period for a representative participant, time-locked to the onset of each stimulation pulse. We observed a sustained cluster of activity throughout the theta band wherein power increased with consecutive TS stimulation pulses ($r = 0.08$, $p < 0.001$, permutation test, family-wise error rate (FWE) corrected). PB stimulation in the same participant showed the opposite effect (Fig. 2A, bottom) wherein theta power decreased with additional stimulation ($r = -0.07$, $p = 0.002$, permutation test, FWE corrected).

We next assessed whether these relative power increases during TS stimulation were consistent across individuals (Fig. 2C). After normalizing theta power to the beginning of the repetitive stimulation period, we found hippocampal theta oscillations increased in amplitude over the course of TS stimulation ($t(3) = 3.8$, $p = 0.03$, $g = 1.9$, 95%

https://doi.org/10.1038/s41467-025-59417-7

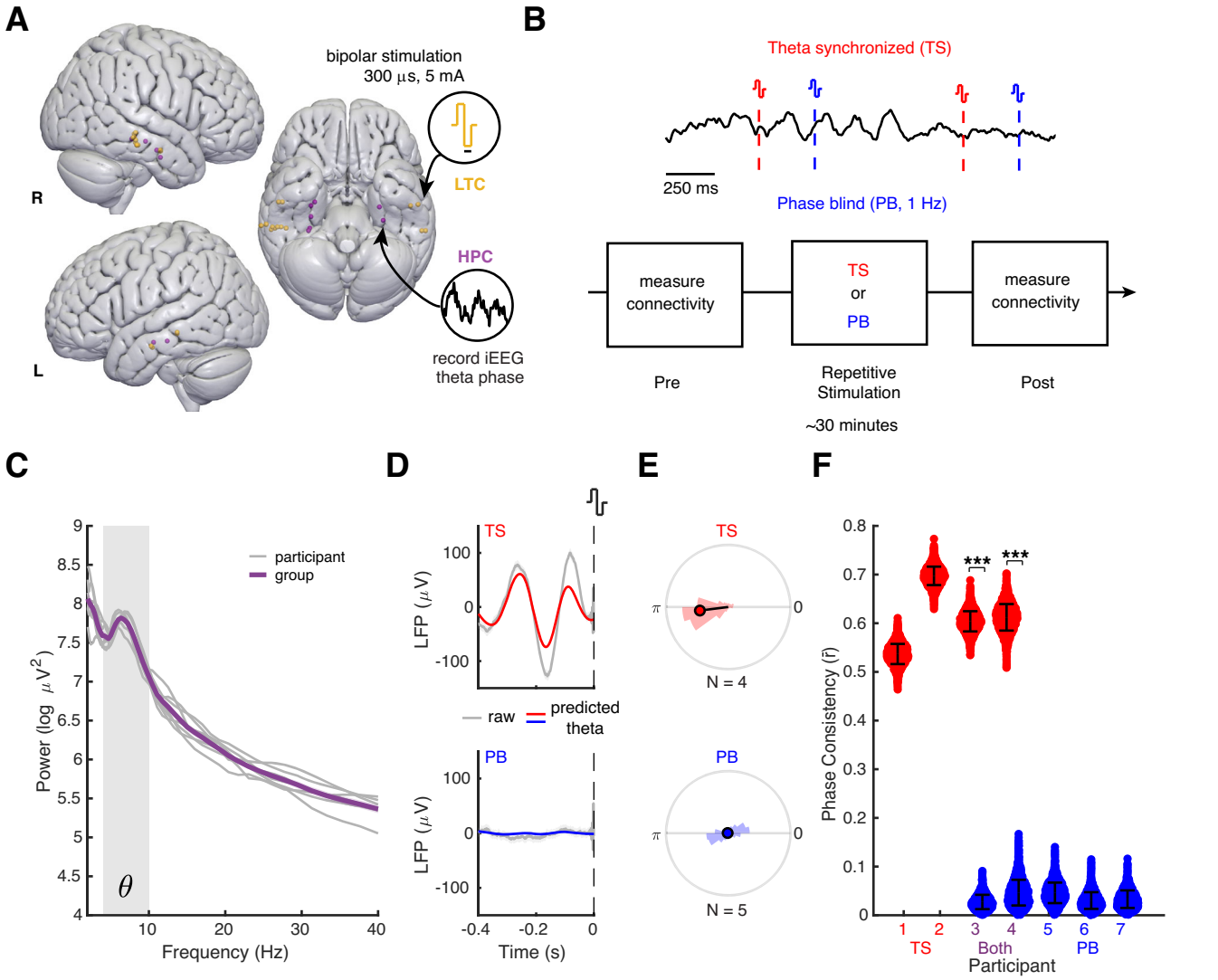

Fig. 1 | Closed-loop stimulation of the hippocampal network. A Stimulation was delivered to network nodes in the lateral temporal cortex (LTC) while theta phase was recorded in real-time from the hippocampus (HPC). **B** For theta-synchronized stimulation (TS), LTC stimulation pulses separated by greater than 1000 ms were phase-synchronized to the trough of hippocampal theta using closed-loop control. Phase-blind stimulation (PB) of LTC was delivered at approximately the same rate but without phase synchronization to hippocampal theta. Network connectivity was measured Pre and Post 30 minutes of repetitive TS or PB stimulation. **C** Hippocampal power spectra included theta oscillations (θ, 4–10 Hz, gray shading) present in individual participants (gray lines) and across the group (black line) during pre-stimulation rest. **D** Example session (participant 2) illustrating the average theta-filtered hippocampal local field potential (LFP) just prior to TS (1007 stimulation events, red trace) and PB stimulation (1142 stimulation events, blue trace). Unfiltered traces are shown in gray. The trough at the time of TS stimulation ($t = 0$, dashed line) shows the efficacy of the closed-loop algorithm. **E** The hippocampal theta phase at the time of LTC stimulation during TS (3448 stimulation events from four participants, top histogram in red) and PB stimulation (5302 stimulation events from five participants, bottom histogram in blue). Black lines denote the mean vector of all phases on the unit circle, with TS stimulation occurring during the theta trough (π). **F** Average theta phase consistency ($\bar{r}$) for each participant during TS (red dots) and PB stimulation (blue dots). Error bars denote ± SEM estimated from a bootstrap procedure. Significant differences in the phase consistency of TS and PB stimulation are denoted for participants 3 ($n = 2149$ stimulation events, $U^2 = 7.0$, $p < 0.001$, Watson's two-sample test, one tailed) and 4 ($n = 1112$ stimulation events, $U^2 = 3.0$, $p < 0.001$, Watson's two-sample test, one tailed) by asterisks (***). Source data are provided as a Source Data file.

CI = [0.13, 0.6]) but not PB stimulation ($t(4) = -1.1$, $p = 0.32$, $g = -0.5$, 95% CI = [1.4, 10.2]). Theta power increased significantly during TS versus PB stimulation ($F(1, 4.83) = 12.7$, $p = 0.017$). Exploratory analyses examining the frequency specificity of these effects highlight their presence only in the theta band (Fig. S1A, B). These findings indicate that TS stimulation of LTC caused hippocampal theta entrainment.

We also asked if endogenous theta synchrony between hippocampus and LTC increased throughout the course of TS as compared to PB stimulation. Theta synchrony at 6 Hz (selected based on the interaction effect for power, see Fig. S1) increased during TS stimulation ($t(3) = 11.4$, $p = 0.001$, $g = 5.7$, 95% CI = [1.4, 10.2]) but not PB stimulation ($t(4) = -0.50$, $p = 0.64$, $g = -0.2$, 95% CI = [−1.1, 0.7]). This apparent difference between stimulation conditions was statistically significant ($F(1, 7.32) = 13.7$, $p = 0.007$), providing additional evidence that TS stimulation caused theta entrainment of the cortico-hippocampal network.

If TS stimulation increased network plasticity during the repetitive stimulation period, we would also predict increases in effective connectivity between the LTC and hippocampus throughout this period. To test this prediction, we examined changes in both early (15–50 msec) and late (50–250 msec) SEP amplitude (Fig. 3A, B). Early

https://doi.org/10.1038/s41467-025-59417-7

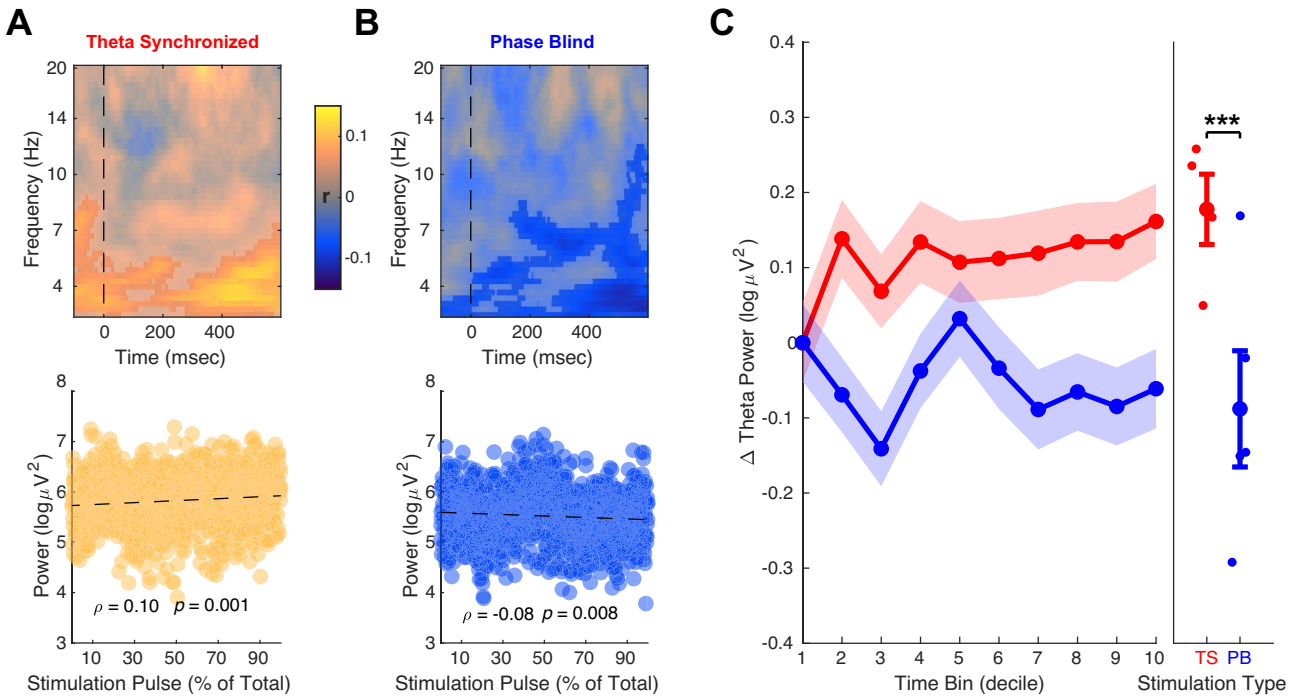

Fig. 2 | Theta-synchronized stimulation increases hippocampal theta. **A** Changes in endogenous theta over the course of repetitive theta-synchronized (TS) in a representative participant. Endogenous theta-band power was computed for the peri-stimulation interval using generalized eigenvalue decomposition to remove stimulation-evoked responses. Endogenous theta power significantly increased over the course of repetitive TS stimulation pulses ($p < 0.05$, FWE corrected, permutation test). Time-frequency pairs with non-significant changes are transparency masked. The vertical dashed line indicates the onset of stimulation. The scatter plot below depicts a significant example from this session ($n = 1007$ stimulation events, Pearson's $r = 0.10$, $p = 0.001$, two-tailed), with each point denoting an individual TS stimulation event. **B** Decreases in endogenous theta power over the course of repetitive phase-blind (PB) stimulation. The participant and plotting convention both follow (**A**), with an example significant effect shown below ($n = 1142$ stimulation events, Pearson's $r = -0.08$, $p = 0.008$, two-tailed). **C** Group mean changes in theta throughout the repetitive stimulation period (±SEM in shaded regions) for TS and PB stimulation. Stimulation pulses were grouped into deciles to account for variability in the number of pulses across subjects (TS stimulation: 40–85 pulses per decile, mean = 58 pulses, PB stimulation: 49–117 pulses per decile, mean = 77 pulses). Endogenous theta power was normalized to the first decile. Endogenous theta power increased during TS versus PB stimulation ($n = 7$ participants, linear mixed-effects model $\beta = 0.08$, 95% CI = [0.02, 0.14], $F(1, 6.8) = 6.4$, $p = 0.04$, ***). Source data are provided as a Source Data file.

SEP amplitude did not change during TS stimulation ($t(3) = 0.8$, $p = 0.48$, $g = 0.4$, 95% CI = [−0.7, 1.4]), or PB stimulation ($t(4) = 0.40$, $p = 0.71$, $g = 0.2$, 95% CI = [−0.7, 1.1]), with no evident differences between the two types of stimulation ($F(1, 42.63) = 0.10$, $p = 0.75$). Although we did not observe differences in late SEP amplitude compared to the first decile of TS ($t(3) = 1.0$, $p = 0.38$, $g = 0.52$, 95% CI = [−0.6, 1.5]) or PB ($t(4 = -2.56$, $p = 0.06$, $g = -1.14$, 95% CI = [−2.3, 0.1]) stimulation (Fig. 3C), late SEP amplitudes increased for TS relative to PB stimulation ($F(1, 4.90) = 17.81$, $p = 0.009$). TS stimulation thus caused immediate increases in both theta and effective connectivity in the hippocampal network, relative to PB control. Taken together, these findings support the hypothesis that repetitive TS stimulation increased network plasticity, potentially leading to persistent changes in connectivity.

Persistent increases in cortico-hippocampal network connectivity following theta-synchronized stimulation

>We next tested whether TS stimulation persistently affected cortico-hippocampal network connectivity. As described above, SPES to the LTC generated SEPs in the hippocampus (Fig. 4A). Like the SEPs collected during repetitive stimulation, SEP waveforms displayed multiphasic responses with an early positivity (P1) peaking at 30 (±0.2) ms, followed by an early negative component (N1) peaking at 131 (±1.1) ms, and a later positive component (P2) peaking at 159 (±5.5) ms following stimulation. SEP waveforms were more variable following PB stimulation, and did not demonstrate the prominent increases in late-waveform amplitude following repetitive stimulation (Fig. 4B). We compared the effects of TS and PB stimulation on both of these components. As shown in Fig. 4C, we observed an increase in SEP amplitude following stimulation for the late ($F(1, 60.70) = 5.77$, $p = 0.02$) but not early waveform components ($F(1, 705.58) = 0.13$, $p = 0.72$) relative to PB control. These effects could not be attributed to between-condition differences prior to repetitive stimulation (see Fig. S3), as we found no evidence for an effect of stimulation condition ($F(1, 3.1) = 3.3$, $p = 0.16$) or an interaction between stimulation condition and waveform timing (early, late; $F(1, 3.7) = 6.0$, $p = 0.08$). The observed differences in late SEP amplitude implicate indirect rather than direct connections driving the hippocampal response to stimulation[43].

We additionally assessed the effects of stimulation on network connectivity by measuring changes in theta synchrony between LTC and hippocampus during rest periods immediately prior to (Pre) and following (Post) the 30 min period of repetitive TS or PB stimulation. Given prominent theta oscillations centered at 5 Hz (Fig. 1C), we expected changes in synchrony would occur at this peak frequency. As shown in Fig. 4D, connectivity between these hippocampal network nodes increased following TS to a greater extent than following PB stimulation (time × stimulation interaction, $F(1, 11.55) = 5.82$, $p = 0.03$). We did not observe significant main effects of time (pre vs. post, $F(1, 6.4) = 1.49$, $p = 0.26$) or stimulation condition (TS vs. PB, $F(1, 6.68) = 0.02$, $p = 0.88$) on network coherence. This specific increase to connectivity following TS stimulation suggests phase-dependent stimulation may be a more effective means to modulate hippocampal networks.

Given our interest in testing the communication-through-coherence hypothesis[9,44] and that our findings are potentially impacted by our choice of synchronization measure, we repeated the aforementioned analyses using the classic magnitude-squared coherence[49]. There were no significant main effects of condition (all $p > 0.25$) or time × stimulation interaction (all $p > 0.40$) on coherence within the theta range. However, it is well known that coherence is susceptible to the effects of volume conduction because it is sensitive to zero-lag synchronization. It is therefore common to also consider the imaginary part of coherence, which discounts zero-lag synchronization and is therefore not sensitive to volume conduction[50]. The effects on PLI reported above were replicated when measuring neural synchronization using the imaginary part of coherence. We found a greater increase in the imaginary part of coherence for TS relative to PB stimulation ($F(1, 11.58) = 10.38$, $p = 0.008$), with no significant main effects of time (pre vs. post, $F(1, 3.71) = 5.01$, $p = 0.09$) or stimulation condition (TS vs. PB, $F(1, 3.12) = 0.70$, $p = 0.46$). As such, our findings of enhanced connectivity are not due to a specific measure of neuronal synchronization. However, the presence of zero-lag synchronization (potentially due to volume conduction or reference activity) likely obscured these effects when using magnitude-squared coherence.

Numerous additional processes could contribute to greater connectivity following theta-synchronized stimulation. With regards to increased effective connectivity (measured by SEPs in the hippocampus), the excitation–inhibition (E–I) balance in the hippocampus could have shifted towards a more excitable regime following network-targeted stimulation, resulting in greater early amplitudes of evoked potentials[42]. Similarly, stimulation could increase the prevalence or amplitude of theta oscillations across the hippocampal network (i.e., in both LTC and hippocampus), leading to greater network coherence. To test these alternative accounts, we fitted hippocampal power spectra as a combination of periodic (i.e., putative oscillations) and aperiodic components[51], and then asked whether stimulation influenced theta oscillations and E–I balance within the network.

We observed roughly equivalent theta oscillations before versus after the TS and PB conditions in hippocampus and LTC (Fig. S2A). There was no evidence that stimulation generally affected theta oscillations ($F(1, 10.6) = 0.8$, $p = 0.40$) or caused condition-specific effects on theta ($F(1, 7.6) = 1.7$, $p = 0.23$) in the hippocampus or LTC at this timescale. E–I balance, approximated by the slope of the power spectrum[52], was similarly unaffected by stimulation (Fig. S2A, B). We found no evidence for an effect of stimulation ($F(1, 4.1) = 0.6$, $p = 0.49$) or a difference between theta-synchronized and control stimulation ($F(1, 3.5) = 1.6$, $p = 0.28$). As was the case with hippocampal activity, stimulation had no apparent effect on this metric of E–I balance in LTC (Fig. S2C, D; see Table S2 for details). These findings suggest TS stimulation caused persistent changes in network connectivity rather than affecting local activity states in the sites of direct LTC or indirect (hippocampus) stimulation.

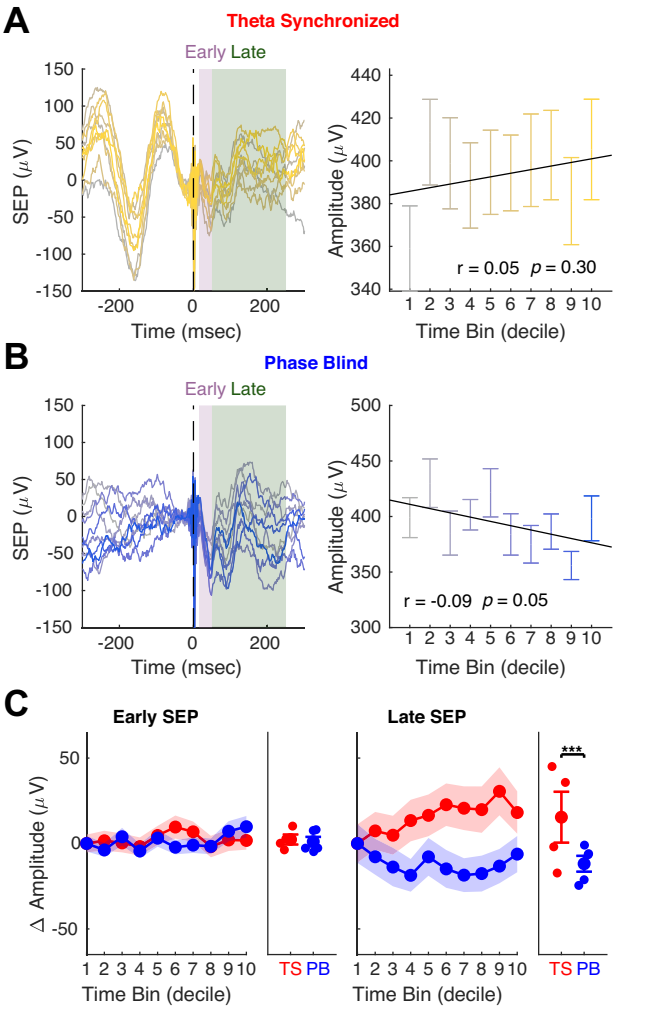

Fig. 3 | Theta-synchronized stimulation increases hippocampal network connectivity. A Changes in stimulation-evoked potential (SEP) amplitude over the course of theta-synchronized (TS) and phase-blind (PB) stimulation periods. Representative data are from the same participant shown in Fig. 2A. Left, SEPs averaged over each decile of TS stimulation pulses (10% of the total number of pulses per decile, color intensity increases with time). Right, late (50–250 msec) peak-to-peak SEP amplitude remained relatively stable ($n = 400$ stimulation events, Pearson's $r = 0.05$, $p = 0.30$, two-tailed) during TS stimulation (error bars denote ± SEM). **B** Changes in SEP amplitude from the same participant decreased during PB stimulation across deciles. Plotting convention follows (**A**), with a non-significant decrease in amplitude over time ($n = 490$ stimulation events, Pearson's $r = -0.09$, $p = 0.05$, two-tailed). **C** Group mean changes in theta throughout the repetitive stimulation period (±SEM in shaded regions) for TS and PB stimulation. Stimulation pulses were grouped into deciles to account for variability in the number of pulses across subjects (see Fig. 2 for details). Changes in SEP amplitude were normalized to the first decile. Left, early (15–50 msec) peak-to-peak SEP amplitude did not vary across TS or PB stimulation across the group. Right, late peak-to-peak SEP amplitude increased for TS stimulation vs. PB control ($n = 7$ participants, linear mixed-effect model $\beta = 18.6$, 95% CI = [9.8, 27.3], $F(1, 4.9) = 17.8$, $p = 0.009$, ***). Source data are provided as a Source Data file.

Discussion

To test whether theta oscillations modulate cortico-hippocampal network connectivity, we applied theta-synchronized stimulation to regions of LTC located within the hippocampal network and examined the impact on neuronal activity and network coupling as compared to a phase-blind control condition. Theta-synchronized stimulation enhanced hippocampal theta oscillations, late SEP waveform amplitude in hippocampus, and theta synchrony between hippocampus and LTC throughout the period when it was applied. This enhanced network connectivity persisted for minutes following stimulation. Multiple measures of excitability did not show such immediate or lasting effects. Early SEP waveform amplitude increased following TS stimulation, but did not differ from control stimulation. These findings demonstrate that the timing of ongoing theta oscillations determines the ultimate impact of stimulation on network physiology, providing a pathway to affect cognitive functions that depend on hippocampal theta.

We provide evidence that theta oscillations can impact communication between brain regions. The communication through coherence theory of inter-regional communication proposes that communication between brain regions is enhanced when synaptic inputs from distant regions arrive at the excitable phase of a neuronal

https://doi.org/10.1038/s41467-025-59417-7

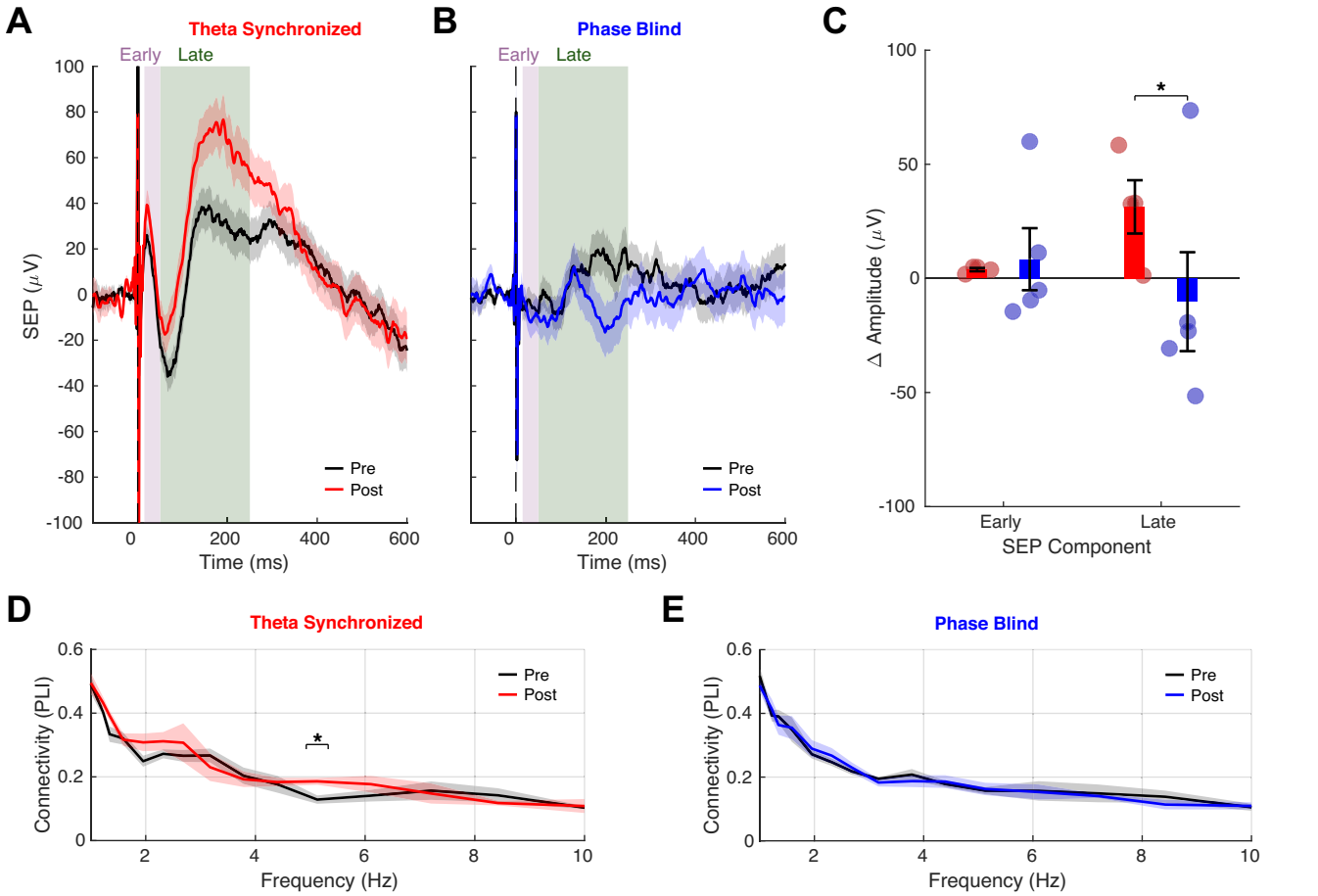

Fig. 4 | Theta-synchronized (TS) stimulation persistently increased SEP and PLI metrics of network connectivity. A Mean SEPs before (Pre) and after (Post) TS stimulation (onset at $t = 0$, dashed line). **B** Mean SEPs following phase-blind (PB) control stimulation. Plotting conventions follow (**A**). **C** Mean changes (post vs. pre) in peak-to-peak waveform amplitude for early and late time periods. TS stimulation increased SEP amplitude compared to PB stimulation ($n = 7$ participants, linear mixed-effects model $\beta = 10.3$, 95% CI = [1.9, 18.7], $F(1, 60.7) = 5.8$, $p = 0.02$, *). **D** Mean phase lag index (PLI) before (Pre) and after (Post) TS stimulation. Significant increases following TS stimulation are denoted by asterisks ($n = 7$ participants, linear mixed-effects model $\beta = 0.01$, 95% CI = [0.003, 0.03], $F(1, 11.5) = 5.8$, $p = 0.03$, *). **E** Mean PLI before (Pre) and after (Post) shows no observable effect of PB stimulation. **A**–**E** Black lines denote Pre, red lines denote Post TS stimulation, and blue lines denote Post PB stimulation. Shaded regions and error bars denote ± SEM. Source data are provided as a Source Data file.

population[9]. Multiple mechanisms can modulate communication between connected regions, including oscillatory shifts that phase-align oscillations to optimal delays or shifts in the synchrony between brain regions without a phase shift[44]. Observational studies of hippocampal dynamics in primates are broadly consistent with synchrony supporting inter-regional communication. For example, increased synchrony between the hippocampus and MTL cortex[53], perirhinal cortex[54], and retrosplenial complex[55] is associated with distinct memory processes.

However, such correlational studies do not imply a causal mechanism. Alternative theories can equally account for these findings, including coherence through communication[10] which describes coherence as epiphenomenal to signal transmission between brain regions. Rather, synchrony between regions results from oscillatory inputs to and local interactions within a region. Both the strength of synaptic coupling and oscillatory power in the sending region have profound impacts on coherence[56]. Our findings are incompatible with this theory, as enhanced hippocampal network synchrony increased without concomitant changes in theta power in LTC. Our findings are also broadly incompatible with communication through resonance[57], in which resonant properties of the receiving region (i.e., the hippocampus in our protocol) produce coherent activity even in the absence of oscillatory inputs, as we observed no lasting change in hippocampal theta. Rather than the phase of inputs, the amount of energy at the resonant peaks determines the strength of coherence. Our findings of strengthened connectivity but equivocal aperiodic and theta power following theta-synchronized stimulation are inconsistent with this mechanism. Our findings instead support a process by which theta-synchronized stimulation led to entrainment of the hippocampal network, leading to lasting, enhanced network connectivity reflected in modulations of oscillatory synchrony and enhanced SEPs.

Our findings have two primary advantages that overcome the limitations of previous work that examined synchrony in hippocampal networks[6,54]. First, we demonstrate both causal (SEP) and correlational (synchrony) changes in hippocampal network connectivity, ruling out the possibility that changes in network connectivity are epiphenomenal. Second, we demonstrate changes in connectivity across the hippocampal network in the absence of a cognitive task. Although some may consider this a disadvantage in understanding how stimulation could affect memory function, interpreting the effects of stimulation on the brain during ongoing behavior has inferential limitations. That is, it can be difficult to disambiguate the effects of stimulation itself from the downstream effects on behavior-related activity. Future studies should examine whether theta-synchronized stimulation can directly impact ongoing memory function. Evidence from animal models shows that closed-loop stimulation to modulate fronto-hippocampal circuits impacts memory behavior[58]. However, it

remains to be seen whether phase-specific modulation can affect specific hippocampal-dependent behaviors.

This study highlights the importance of the LTC in its capacity to modulate hippocampal networks. In contrast to direct stimulation of the hippocampus and entorhinal cortex that has been shown to impair memory function[59,60] (but see refs. 61,62), noninvasive stimulation of network nodes in the lateral parietal cortex[32,63] and DES of network nodes in the LTC[64,65] have improved memory. Our findings suggest that the effects of LTC stimulation in the hippocampus are the result of network-based interactions, consistent with previous studies showing that the effects of DES are determined by large-scale brain networks[6,33,66]. Advances in precision mapping of mesial-temporal networks have identified sites in the LTC that belong to an entorhinal network[8], suggesting a specific pathway to influence the hippocampus.

Our findings suggest that phase-synchronized stimulation may have a greater impact on network communication than on individual network nodes. Whereas evoked potentials in the hippocampus were enhanced by TS stimulation, readouts of cortical excitability (1/*f* exponent, low-frequency desynchronization, and early SEP amplitude) showed no apparent effects specific to TS stimulation. Measuring the amplitude or slope of the evoked response to electrical stimulation is widely held as a measurement of cortical excitability[67,68], including noninvasive applications in measuring motor-evoked potentials or potentials in scalp EEG following noninvasive transcranial magnetic stimulation[69]. Although TS stimulation increased the amplitude of early SEP responses, this effect was not convincingly different from control stimulation. We believe that variability in stimulation sites could contribute to this null finding, as control stimulation occurred more frequently in the posterior portions of LTC with less direct hippocampal connectivity[70]. Future studies that target direct hippocampal inputs in combination with single-unit recordings to assess changes in excitability could help clarify the effect of TS stimulation on excitability. Despite no evidence for changes in excitability, our findings of network-based effects converge with recent studies that show oscillations control network plasticity and inter-regional communication[39], with network dynamics controlling signal transmission[71].

A focus of many approaches to brain stimulation is to deliver exogenous stimulation using rhythmic patterns that mimic the endogenous brain rhythms[30]. Thus, prominent approaches to affect memory circuits have involved theta frequency stimulation[15,72,73] or theta-burst stimulation in which bursts of high frequency stimulation are nested within the theta rhythm[13,14,16,74,75], as theta and theta-nested gamma are endogenous to the hippocampus. Although theta enhancement has been demonstrated using these approaches[16,54], stimulation has been limited to medial temporal lobe structures and proximal white matter (but see ref. 75). Our findings suggest effectiveness of a more nuanced approach to network-targeted stimulation. We demonstrate that closed-loop phase synchronization, which tunes into endogenous network oscillations, significantly yields entrainment. This method contrasts with the traditional approach of imposing an external rhythmic pattern and instead enhances intrinsic rhythmicity, offering new insights into the mechanisms of brain stimulation and its potential therapeutic applications.

Our study has several limitations. Theta-synchronized stimulation was restricted to the theta trough due to practical constraints. Our decision to stimulate at theta trough was motivated by findings of network plasticity during the trough (depolarizing phase) of oscillations[39] and greater evoked potentials in the hippocampus when LTC stimulation is delivered at theta trough[25]. Future studies will be necessary to determine whether there are optimal phases to affect connectivity of hippocampal networks and whether these phases vary across anatomical regions and memory processes (i.e., during encoding versus retrieval[76,77]). In addition, our study was limited to a rather small sample of neurosurgical patients. As a result, we were only able to study a restricted set of nodes within the cortico-hippocampal network. Another limitation is the fact that our study was conducted in patients with epilepsy, raising the possibility that our findings may not generalize to the healthy brain. We took a number of steps to limit related concerns. Both stimulation sites in the LTC and phase-determining sites in the hippocampus were outside the seizure-onset zone. Stimulation amplitudes were selected to avoid epileptiform discharges, which were also excluded from analysis when they spontaneously occurred.

To conclude, we show that theta-synchronized stimulation entrains the human cortico-hippocampal network, producing lasting increases in network connectivity. Enhanced network coupling persisted in the absence of increased hippocampal inputs from the LTC, lasting changes in theta power, or modulations in the balance of excitation and inhibition across the network. These findings show that theta phase modulates connectivity across hippocampal networks, supporting theories in which oscillations play a causal role in inter-regional communication. Stimulation synchronized to the theta rhythm thus provides an effective means to modulate hippocampal network function.

Methods

Participants

Seven patients (two females) undergoing intracranial electroencephalographic recordings to monitor for seizures were recruited to participate in the study. A subset of data from four participants was included in an earlier publication examining the effects of theta phase on evoked potentials in the hippocampus[25], but the effects of phase-locked stimulation were not previously analyzed. Data from the remaining patients have not been published, and all of the reported analyses examining the effects of theta-synchronized stimulation are novel. Data were collected at Northwestern Memorial Hospital (Chicago, IL) and the University of Chicago Medical Center (Chicago, IL). The research protocol was approved by the Institutional Review Boards of the University of Chicago and Northwestern University, and informed consent was given by each participant.

iEEG recordings

Stereotactic EEG electrodes (contacts spaced 5–10 mm apart, AD-TECH Medical Instrument Co., Racine, WI) and subdural grids and/or strips (contacts spaced 10 mm apart) targeted brain structures to localize epileptogenic tissue and provided additional coverage in hippocampus and LTC outside seizure networks. Electrophysiological signals were recorded using the Neuralynx ATLAS recording system (Bozeman, MT), at a sampling rate of 30 kHz using a clinical reference and ground consisting of either scalp electrodes or an implanted electrode strip facing the scalp. Prior to analysis, recorded signals were bandpass-filtered from 0.1 to 1 kHz and resampled to 500 Hz. Line noise and harmonics were removed with a discrete Fourier transform filter. To exclude inter-ictal epileptiform discharges and other noise sources, epochs were excluded on a per-analysis basis using an absolute amplitude threshold of 500 μV, a kurtosis threshold of five, and a normalized amplitude threshold of five standard deviations.

Electrode localization

Postimplant computed tomography (CT) images were coregistered to pre-surgical T1-weighted structural MRIs using SPM12[78]. T1-weighted MRI scans were normalized to MNI (Montreal Neurological Institute) space by using a combination of affine and nonlinear registration steps, bias correction, and segmentation into gray matter, white matter, and cerebrospinal fluid components[79]. Deformations from the normalization procedure were applied to individual electrode locations identified on postimplant CT images using Bioimage Suite[80]. For subdural grids and strips, electrode locations were snapped to the

cortical surface using an energy minimization algorithm to account for brain shifts[81].

Stimulation protocol

At the start of each session, we determined the safe amplitude for stimulation using a mapping procedure in which 10 single pulses of stimulation were applied at 1 mA at 0.5 Hz, while a neurologist monitored for afterdischarges. This procedure was repeated, incrementing the amplitude in steps of 1 mA, up to a maximum of 5 mA (well below accepted safety limits for charge density[82]). When multiple sites in LTC were available for stimulation, the site that produced the largest magnitude SEP in the hippocampal electrode used for phase-locking over 20 single pulses, applied at 0.5 Hz, was selected as the site of stimulation. Sites were selected via visual inspection or online averaging of hippocampal traces. Phase-locking sites in hippocampus were selected based on visual observation of theta in continuous EEG prior to each session. Stimulation was tolerated well by all seven participants, none of whom showed afterdischarges following initial 5 mA stimulation. Of note, stimulation sites were selected following clinical mapping and determination of the seizure-onset zone, and these regions were excluded as stimulation sites.

For each stimulation session, we passed electrical current through a single pair of adjacent electrode contacts in LTC. Stimulation was delivered using charge-balanced biphasic rectangular pulses (pulse width = 300 µs, inter-pulse interval = 53 µs) at an amplitude of 5 mA. Stimulation waveforms were generated using either a Grass Instruments S88 (with constant current units and stimulus isolators) or a CereStim R96 (Blackrock Microsystems) delivering stimulation in true bipolar mode (i.e., with one channel in the bipolar pair linked to the stimulator ground).

During each session, subjects rested quietly and did not perform any task. Each session consisted of a 30-minute repetitive stimulation period (either theta-synchronized or phase-blind stimulation), preceded and followed by a two-minute stimulation-based network mapping protocol (SPES at 0.5 Hz) and a five-minute rest period (Fig. 1B). During the theta-synchronized condition, stimulation was timed to coincide with the trough of hippocampal theta oscillations using closed-loop control. Using TORTE within Open Ephys[45,83] on a control PC, continuous neural data streamed from the Neuralynx ATLAS were causally filtered through a 2nd-order Butterworth filter (4–10 Hz) and downsampled to 500 Hz. Assuming frequency stationarity over the short buffer, a 20th-order autoregressive model then predicted the upcoming theta-band signal. A Hilbert transformer then computed the analytic signal for observed and predicted data segments, allowing a learning algorithm to optimize the timing of stimulation based on round-trip latency of the system[45]. Similar routines were applied offline in MATLAB (r2023a, Natick, MA) to evaluate the accuracy of the system.

During theta-synchronized stimulation, the learning algorithm determined a phase-lag to reliably time stimulation to the trough of hippocampal theta. An additional constraint was set such that two consecutive stimulation events were separated by at least one second, preventing stimulation artifact or evoked responses from affecting phase estimation. Our control condition consisted of phase-blind stimulation at 1 Hz, timed to match the minimum delay between consecutive stimulation events. Stimulation events were logged via analog TTL pulses delivered at the onset of stimulation.

Stimulation-based connectivity estimation

To evaluate effective connectivity between the LTC and the hippocampus, we recorded evoked potentials following SPES delivered to the LTC. SPES involved delivering single pulses (with parameters described as above) and measuring the SEPs across all recorded sites, with particular focus on recording sites within the hippocampus. SPES provides insights into the strength and direction of connections between stimulated and recorded sites[37]. Following successful approaches to map hippocampal connectivity in this way[40,43,84], we examined the amplitude of early evoked waveforms thought to reflect direct connections between stimulated and measured areas[34,36]. To account for multiphasic waveforms, we computed peak-to-peak amplitude during early waveform components from 15–50 ms after stimulation. In addition, we measured late-going waveform components by computing the peak-to-peak amplitude from 50–250 msec after stimulation. To account for low-frequency drifts, SEPs were corrected to a baseline period (−50 to −10 msec relative to stimulation onset).

Synchrony-based connectivity estimation

To estimate functional connectivity between the LTC and hippocampus during rest, we used the PLI. PLI is sensitive to detect changes in phase synchronization while discounting the influence of common sources, volume conduction, and active reference electrodes[48]. We selected PLI to measure neuronal synchronization because, unlike measures such as coherence that reflect both amplitude covariation and phase alignment[85], PLI only measures phase alignment between two signals. As such, PLI will discount amplitude covariation during transient, high-amplitude signals containing energy in the theta frequency range (e.g., epileptiform activity). PLI is defined as:

$$PLI = |<sign[\Delta\phi(t_{x,y})]>|, \tag{1}$$

where $\Delta\phi(t_{x,y})$ represents the phase difference between two channels (x, y) at time t, which was computed via Morlet wavelet decomposition (cycle number = 6). Five-minute rest periods were epoched into multiple 8-s trials duration, with 80% of overlap across consecutive trials. We also compared this measure of neural synchronization to the magnitude-squared coherence[49] and the imaginary part of coherence, which has better properties for dealing with volume conduction[50]. For these measures, epochs were increased to 10 seconds in duration, with 90% overlap over consecutive trials. The coherence between two signals $x(t)$ and $y(t)$ is defined as:

$$C_{xy} = \frac{|S_{xy}|^2}{S_{xx}S_{yy}}, \tag{2}$$

where S_{xy} is the cross-spectral density, and S_{xx} and S_{yy} are the power spectral densities of the two signals. Following the same notation, the imaginary (Im) part of coherence is defined as:

$$\mathrm{Im}(C_{xy}) = \frac{\mathrm{Im}\,(S_{xy})}{\sqrt{S_{xx}S_{yy}}} \tag{3}$$

Stimulation-evoked changes in theta power

In order to examine the immediate effects of closed-loop stimulation on theta oscillations, we used generalized eigenvalue decomposition (GED) as a source separation technique to remove artifactual and other signals time-locked to the onset of stimulation[47]. In brief, we used GED to optimize a spatial filter (i.e., a set of linear weights across recording channels) to maximize a contrast between SEPs and other signals time-locked to stimulation and endogenous or induced (phase random) activity. We considered data from 50 ms prior to 800 ms after repetitive stimulation events (i.e., phase-blind stimulation or theta-synchronized stimulation) and computed a spatial filter ($\mathbf{w}$) that maximized $\mathbf{\Lambda}$ to extract stimulation-locked features of the signal:

$$\mathbf{\Lambda} = \frac{\mathbf{w}^\top \mathbf{S}\mathbf{w}}{\mathbf{w}^\top \mathbf{R}\mathbf{w}}, \tag{4}$$

where **S** is the covariance matrix computed from the trial-averaged response to stimulation and **R** is the mean of the single-trial covariance matrices[86,87]. Any source that explained at least (1%) of the trial-averaged response was filtered from the EEG timeseries. Theta activity in the cleaned EEG timeseries was computed using Morlet wavelet decomposition and baselined to the first 10% of stimulation events during the repetitive stimulation period.

Power spectrum parameterization

To test whether the theta-synchroinzed stimulation affected either the balance of excitation to inhibition or the magnitude of theta oscillations, we modeled the aperiodic and putative oscillatory (i.e., periodic) components of the power spectra. Following prior work[51,88], we fitted the aperodic component (A) using a Lorentzian function:

$$A = b - log(k + F^{\alpha}), \quad (5)$$

where b is the broadband offset, α is the exponential decay, and k is the 'knee' parameter that reflects the speed of neuronal timescales[89]. We fitted these parameters to data from rest epochs before and after the 30-minute repetitive stimulation periods, examining frequencies ranging from 2 to 40 Hz. The fitting procedure was robust to periodic signals present in the data as it excluded frequencies where the original spectra exceeded a power threshold (2.5 $\log(\mu V^2)$) from an initial aperiodic fit. We used the α parameter as an index of the excitation-to-index ratio[52] and the average power in the theta band (4–9 Hz) after subtracting out the aperiodic component of the signal.

Linear mixed-effects models

For statistical analysis, we used linear mixed-effects models to account for subject-level variability as well as variation related to closed-loop stimulation. Our primary analyses examined the effects of stimulation type (theta synchronized vs. phase blind) on connectivity of the hippocampal network over time (pre vs. post). Separate models were fitted for measures of effective connectivity (to SEP amplitude) and coherence (to PLI). The full model was specified in MATLAB as:

$$\text{conn} \sim \text{stim*time} + (\text{stim*time}|\text{subject}). \quad (6)$$

The same modeling approach was used to examine changes in theta power and SEP amplitude over the course of the repetitive stimulation period, using the appropriate dependent measure. For inference on linear mixed-effects models, Satterthwaite approximations[90] were used to estimate degrees of freedom, and effects were considered significant at $\alpha = 0.05$, two-tailed.

Reporting summary

Further information on research design is available in the Nature Portfolio Reporting Summary linked to this article.

Data availability

The experimental data generated in this study are available through OpenNeuro[91] (https://doi.org/10.18112/openneuro.ds006065.v1.0.0). The data to reproduce all figures are available in a source data file.

Code availability

The code to run closed-loop stimulation is freely available[92] (https://doi.org/10.5281/zenodo.5539831). Additional code to reproduce all results is available through Zenodo[93] (https://doi.org/10.5281/zenodo.14735080).

References

1. Buzsáki, G. Theta oscillations in the hippocampus. *Neuron* **33**, 325–340 (2002).
2. Buzsáki, G. Theta rhythm of navigation: link between path integration and landmark navigation, episodic and semantic memory. *Hippocampus* **15**, 827–840 (2005).
3. Colgin, L. L. Mechanisms and functions of theta rhythms. *Annu. Rev. Neurosci.* **36**, 295–312 (2013).
4. Herweg, N. A., Solomon, E. A. & Kahana, M. J. Theta oscillations in human memory. *Trends Cogn. Sci.* **24**, 208–227 (2020).
5. Fell, J. & Axmacher, N. The role of phase synchronization in memory processes. *Nat. Rev. Neurosci.* **12**, 105–118 (2011).
6. Solomon, E. A. et al. Widespread theta synchrony and high-frequency desynchronization underlies enhanced cognition. *Nat. Commun.* **8**, 1–14 (2017).
7. Barnett, A. J. et al. Intrinsic connectivity reveals functionally distinct cortico-hippocampal networks in the human brain. *PLoS Biol.* **19**, e3001275 (2021).
8. Reznik, D., Trampel, R., Weiskopf, N., Witter, M. P. & Doeller, C. F. Dissociating distinct cortical networks associated with subregions of the human medial temporal lobe using precision neuroimaging. *Neuron* **111**, 2756–2772.e7 (2023).
9. Fries, P. A mechanism for cognitive dynamics: neuronal communication through neuronal coherence. *Trends Cogn. Sci.* **9**, 474–480 (2005).
10. Schneider, M. et al. A mechanism for inter-areal coherence through communication based on connectivity and oscillatory power. *Neuron* **109**, 4050–4067 (2021).
11. Siegle, J. H. & Wilson, M. A. Enhancement of encoding and retrieval functions through theta phase-specific manipulation of hippocampus. *eLife* **3**, e03061 (2014).
12. Scott, L. et al. Age-dependent disruption in hippocampal theta oscillation in amyloid-overproducing transgenic mice. *Neurobiol. Aging* **33**, 1481.e13–1481.e23 (2012).
13. Titiz, A. S. et al. Theta-burst microstimulation in the human entorhinal area improves memory specificity. *eLife* **6**, e29515 (2017).
14. Inman, C. S. et al. Direct electrical stimulation of the amygdala enhances declarative memory in humans. *Proc. Natl. Acad. Sci. USA* **115**, 98–103 (2018).
15. Solomon, E. A. et al. Medial temporal lobe functional connectivity predicts stimulation-induced theta power. *Nat. Commun.* **9**, 4437 (2018).
16. Solomon, E. A. et al. Theta-burst stimulation entrains frequency-specific oscillatory responses. *Brain Stimul.* **14**, 1271–1284 (2021).
17. Kucewicz, M. T., Worrell, G. A. & Axmacher, N. Direct electrical brain stimulation of human memory: lessons learnt and future perspectives. *Brain* **146**, 2214–2226 (2023).
18. Alagapan, S. et al. Modulation of cortical oscillations by low-frequency direct cortical stimulation is state-dependent. *PLoS Biol.* **14**, e1002424 (2016).
19. Lefebvre, J., Hutt, A. & Fröhlich, F. Stochastic resonance mediates the state-dependent effect of periodic stimulation on cortical alpha oscillations. *eLife* **6**, e32054 (2017).
20. Ezzyat, Y. et al. Direct brain stimulation modulates encoding states and memory performance in humans. *Curr. Biol.* **27**, 1251–1258 (2017).
21. Geschwill, P. et al. Synchronicity of excitatory inputs drives hippocampal networks to distinct oscillatory patterns. *Hippocampus* **30**, 1044–1057 (2020).
22. Bradley, C., Nydam, A. S., Dux, P. E. & Mattingley, J. B. State-dependent effects of neural stimulation on brain function and cognition. *Nat. Rev. Neurosci.* **23**, 459–475 (2022).
23. Geva-Sagiv, M. et al. Augmenting hippocampal–prefrontal neuronal synchrony during sleep enhances memory consolidation in humans. *Nat. Neurosci.* **26**, 1100–1110 (2023).
24. Schomburg, E. W. et al. Theta phase segregation of input-specific gamma patterns in entorhinal-hippocampal networks. *Neuron* **84**, 470–485 (2014).

25. Lurie, S. M., Kragel, J. E., Schuele, S. U. & Voss, J. L. Human hippocampal responses to network intracranial stimulation vary with theta phase. *eLife* **11**, e78395 (2022).
26. Huerta, P. T. & Lisman, J. E. Bidirectional synaptic plasticity induced by a single burst during cholinergic theta oscillation in CA1 in vitro. *Neuron* **15**, 1053–1063 (1995).
27. Paulsen, O. & Sejnowski, T. J. Natural patterns of activity and long-term synaptic plasticity. *Curr. Opin. Neurobiol.* **10**, 172–180 (2000).
28. Hyman, J. M., Wyble, B. P., Goyal, V., Rossi, C. A. & Hasselmo, M. E. Stimulation in hippocampal region CA1 in behaving rats yields long-term potentiation when delivered to the peak of theta and long-term depression when delivered to the trough. *J. Neurosci.* **23**, 11725–11731 (2003).
29. Quirk, C. R. et al. Precisely timed theta oscillations are selectively required during the encoding phase of memory. *Nat. Neurosci.* **24**, 1614–1627 (2021).
30. Hanslmayr, S., Axmacher, N. & Inman, C. S. Modulating human memory via entrainment of brain oscillations. *Trends Neurosci.* **42**, 485–499 (2019).
31. Widge, A. S. & Miller, E. K. Targeting cognition and networks through neural oscillations: next-generation clinical brain stimulation. *JAMA Psychiatry* **76**, 671–672 (2019).
32. Hebscher, M. & Voss, J. L. Testing network properties of episodic memory using non-invasive brain stimulation. *Curr. Opin. Behav. Sci.* **32**, 35–42 (2020).
33. Ezzyat, Y. et al. Functional and anatomical connectivity predict brain stimulation's mnemonic effects. *Cereb. Cortex* **34**, bhad427 (2024).
34. Matsumoto, R. et al. Functional connectivity in the human language system: a cortico-cortical evoked potential study. *Brain* **127**, 2316–2330 (2004).
35. Novitskaya, Y., Dümpelmann, M., Vlachos, A., Reinacher, P. C. & Schulze-Bonhage, A. In vivo-assessment of the human temporal network: evidence for asymmetrical effective connectivity. *NeuroImage* **214**, 116769 (2020).
36. Keller, C. J. et al. Mapping human brain networks with cortico-cortical evoked potentials. *Philos. Trans. R. Soc. B: Biol. Sci.* **369**, 20130528 (2014).
37. Matsumoto, R., Kunieda, T. & Nair, D. Single pulse electrical stimulation to probe functional and pathological connectivity in epilepsy. *Seizure* **44**, 27–36 (2017).
38. Palmigiano, A., Geisel, T., Wolf, F. & Battaglia, D. Flexible information routing by transient synchrony. *Nat. Neurosci.* **20**, 1014–1022 (2017).
39. Zanos, S., Rembado, I., Chen, D. & Fetz, E. E. Phase-locked stimulation during cortical beta oscillations produces bidirectional synaptic plasticity in awake monkeys. *Curr. Biol.* **28**, 2515–2526 (2018).
40. Enatsu, R. et al. Connections of the limbic network: a corticocortical evoked potentials study. *Cortex* **62**, 20–33 (2015).
41. Meisel, C. et al. Intrinsic excitability measures track antiepileptic drug action and uncover increasing/decreasing excitability over the wake/sleep cycle. *Proc. Natl. Acad. Sci.* **112**, 14694–14699 (2015).
42. Keller, C. J. et al. Induction and quantification of excitability changes in human cortical networks. *J. Neurosci.* **38**, 5384–5398 (2018).
43. Valencia, G. O. et al. Signatures of electrical stimulation driven network interactions in the human limbic system. *J. Neurosci.* **43**, 6697–6711 (2023).
44. Fries, P. Rhythms for cognition: communication through coherence. *Neuron* **88**, 220–235 (2015).
45. Schatza, M. J., Blackwood, E. B., Nagrale, S. S. & Widge, A. S. Toolkit for oscillatory real-time tracking and estimation (TORTE). *J. Neurosci. Methods* **366**, 109409 (2022).
46. Cohen, M. X. & Gulbinaite, R. Rhythmic entrainment source separation: optimizing analyses of neural responses to rhythmic sensory stimulation. *NeuroImage* **147**, 43–56 (2017).
47. Cohen, M. X. A tutorial on generalized eigendecomposition for denoising, contrast enhancement, and dimension reduction in multichannel electrophysiology. *NeuroImage* **247**, 118809 (2022).
48. Stam, C. J., Nolte, G. & Daffertshofer, A. Phase lag index: assessment of functional connectivity from multi channel EEG and MEG with diminished bias from common sources. *Hum. Brain Mapp.* **28**, 1178–1193 (2007).
49. Nunez, P. L. et al. Eeg coherency: I: statistics, reference electrode, volume conduction, laplacians, cortical imaging, and interpretation at multiple scales. *Electroencephalogr. Clin. Neurophysiol.* **103**, 499–515 (1997).
50. Nolte, G. et al. Identifying true brain interaction from eeg data using the imaginary part of coherency. *Clin. Neurophysiol.* **115**, 2292–2307 (2004).
51. Donoghue, T. et al. Parameterizing neural power spectra into periodic and aperiodic components. *Nat. Neurosci.* **23**, 1655–1665 (2020).
52. Gao, R., Peterson, E. J. & Voytek, B. Inferring synaptic excitation/inhibition balance from field potentials. *NeuroImage* **158**, 70–78 (2017).
53. Fell, J. et al. Human memory formation is accompanied by rhinal–hippocampal coupling and decoupling. *Nat. Neurosci.* **4**, 1259–1264 (2001).
54. Solomon, E. A., Lega, B. C., Sperling, M. R. & Kahana, M. J. Hippocampal theta codes for distances in semantic and temporal spaces. *Proc. Natl. Acad. Sci.* **116**, 24343–24352 (2019).
55. Hussin, A. T., Abbaspoor, S. & Hoffman, K. L. Retrosplenial and hippocampal synchrony during retrieval of old memories in macaques. *J. Neurosci.* **42**, 7947–7956 (2022).
56. Vinck, M. et al. Principles of large-scale neural interactions. *Neuron* **111**, 987–1002 (2023).
57. Hahn, G., Bujan, A. F., Frégnac, Y., Aertsen, A. & Kumar, A. Communication through resonance in spiking neuronal networks. *PLoS comput. Biol.* **10**, e1003811 (2014).
58. Knudsen, E. B. & Wallis, J. D. Closed-loop theta stimulation in the orbitofrontal cortex prevents reward-based learning. *Neuron* **106**, 537–547 (2020).
59. Jacobs, J. et al. Direct electrical stimulation of the human entorhinal region and hippocampus impairs memory. *Neuron* **92**, 983–990 (2016).
60. Goyal, A. et al. Functionally distinct high and low theta oscillations in the human hippocampus. *Nat. Commun.* **11**, 1–10 (2020).
61. Suthana, N. et al. Memory enhancement and deep-brain stimulation of the entorhinal area. *N. Engl. J. Med.* **366**, 502–510 (2012).
62. Mankin, E. A. et al. Stimulation of the right entorhinal white matter enhances visual memory encoding in humans. *Brain stimul.* **14**, 131–140 (2021).
63. Wang, J. X. et al. Targeted enhancement of cortical-hippocampal brain networks and associative memory. *Science* **345**, 1054–1057 (2014).
64. Kucewicz, M. T. et al. Evidence for verbal memory enhancement with electrical brain stimulation in the lateral temporal cortex. *Brain* **141**, 971–978 (2018).
65. Ezzyat, Y. et al. Closed-loop stimulation of temporal cortex rescues functional networks and improves memory. *Nat. Commun.* **9**, 365 (2018).
66. Fox, K. C. et al. Intrinsic network architecture predicts the effects elicited by intracranial electrical stimulation of the human brain. *Nat. Hum. Behav.* **4**, 1039–1052 (2020).
67. Rall, W. Distinguishing theoretical synaptic potentials computed for different soma-dendritic distributions of synaptic input. *J. Neurophysiol.* **30**, 1138–1168 (1967).
68. Vyazovskiy, V. V., Cirelli, C., Pfister-Genskow, M., Faraguna, U. & Tononi, G. Molecular and electrophysiological evidence for net

synaptic potentiation in wake and depression in sleep. *Nat. Neurosci.* **11**, 200–208 (2008).
69. Pellegrino, G. et al. Assessing cortical excitability with electroencephalography: a pilot study with EEG-iTBS. *Brain Stimul.* **17**, 176–183 (2024).
70. Dalton, M. A., D'Souza, A., Lv, J. & Calamante, F. New insights into anatomical connectivity along the anterior-posterior axis of the human hippocampus using in vivo quantitative fibre tracking. *eLife* **11**, e76143 (2022).
71. Qiao, S., Sedillo, J. I., Brown, K. A., Ferrentino, B. & Pesaran, B. A causal network analysis of neuromodulation in the mood processing network. *Neuron* **107**, 972–985 (2020).
72. Mohan, U. R. et al. The effects of direct brain stimulation in humans depend on frequency, amplitude, and white-matter proximity. *Brain Stimul.* **13**, 1183–1195 (2020).
73. Lech, M. et al. Direct electrical stimulation of the human brain has inverse effects on the theta and gamma neural activities. *IEEE Trans. Biomed. Eng.* **68**, 3701–3712 (2021).
74. Miller, J. P. et al. Visual-spatial memory may be enhanced with theta burst deep brain stimulation of the fornix: a preliminary investigation with four cases. *Brain* **138**, 1833–1842 (2015).
75. Kim, K. et al. Network-based brain stimulation selectively impairs spatial retrieval. *Brain Stimul.* **11**, 213–221 (2018).
76. Hasselmo, M. E., Bodelón, C. & Wyble, B. P. A proposed function for hippocampal theta rhythm: separate phases of encoding and retrieval enhance reversal of prior learning. *Neural Comput.* **14**, 793–817 (2002).
77. Hasselmo, M. E. & Stern, C. E. Theta rhythm and the encoding and retrieval of space and time. *NeuroImage* **85**, 656–666 (2014).
78. Ashburner, J. & Friston, K. Multimodal image coregistration and partitioning–a unified framework. *NeuroImage* **6**, 209–217 (1997).
79. Gaser, C. et al. Cat: a computational anatomy toolbox for the analysis of structural mri data. *Gigascience* **13**, giae049 (2024).
80. Papademetris, X. et al. BioImage suite: an integrated medical image analysis suite: an update. *Insight J.* **2006**, 209 (2006).
81. Dykstra, A. R. et al. Individualized localization and cortical surface-based registration of intracranial electrodes. *NeuroImage* **59**, 3563–3570 (2012).
82. Shannon, R. V. A model of safe levels for electrical stimulation. *IEEE Trans. Biomed. Eng.* **39**, 424–426 (1992).
83. Siegle, J. H. et al. Open Ephys: an open-source, plugin-based platform for multichannel electrophysiology. *J. Neural Eng.* **14**, 045003 (2017).
84. Catenoix, H. et al. Hippocampal-orbitofrontal connectivity in human: an electrical stimulation study. *Clin. Neurophysiol.* **116**, 1779–1784 (2005).
85. Lachaux, J.-P., Rodriguez, E., Martinerie, J. & Varela, F. J. Measuring phase synchrony in brain signals. *Hum. Brain Mapp.* **8**, 194–208 (1999).
86. Dmochowski, J. P., Greaves, A. S. & Norcia, A. M. Maximally reliable spatial filtering of steady state visual evoked potentials. *NeuroImage* **109**, 63–72 (2015).
87. Tanaka, H. & Miyakoshi, M. Cross-correlation task-related component analysis (xtrca) for enhancing evoked and induced responses of event-related potentials. *NeuroImage* **197**, 177–190 (2019).
88. Kragel, J. E. et al. Hippocampal theta coordinates memory processing during visual exploration. *eLife* **9**, e52108 (2020).
89. Gao, R., van den Brink, R. L., Pfeffer, T. & Voytek, B. Neuronal timescales are functionally dynamic and shaped by cortical microarchitecture. *eLife* **9**, e61277 (2020).
90. Satterthwaite, F. E. Synthesis of variance. *Psychometrika* **6**, 309–316 (1941).
91. Kragel, J. E. and Voss, J. TSS iEEG https://doi.org/10.18112/openneuro.ds006065.v1.0.0. (2025).
92. Schatza, M. tne-lab/torte: v1.0 https://doi.org/10.5281/zenodo.5539831. (2021).
93. Kragel, J. E. Code related to: closed-loop control of theta oscillations enhances human hippocampal network connectivity. https://doi.org/10.5281/zenodo.14735080. (2025).

Acknowledgements

We are indebted to the patients and their families for their participation and support. This work was supported by National Institutes of Health Grants R01-NS113804 (J.L.V., J.F.D., and A.S.W.) and R01-MH119384 (A.S.W.). The funders had no role in study design, data collection and analysis, publication decisions, or manuscript preparation.

Author contributions

J.E.K., S.M.L., and J.L.V. designed the study. J.E.K. analyzed data and drafted the manuscript. J.E.K., S.M.L, N.P.I, H.A.H., S.W., J.X.T., P.C.W., S.S., J.M.R., C.Z., M.S., J.F.D., A.S.W., and J.L.V. reviewed and edited the manuscript. J.E.K., M.S., and A.S.W. developed software tools for implementing closed-loop stimulation. J.E.K. and S.M.L. collected data. P.C.W. and J.M.R. performed surgeries. N.P.I., H.A.H., S.W., J.X.T., P.C.W., S.S., and J.M.R. recruited participants and performed clinical duties associated with data collection. J.F.D., A.S.W., and J.L.V. acquired funding and supervised the work.

Competing interests

The authors declare no competing interests.

Additional information

Supplementary information The online version contains supplementary material available at https://doi.org/10.1038/s41467-025-59417-7.

Correspondence and requests for materials should be addressed to James E. Kragel.

Peer review information *Nature Communications* thanks Michal Kucewicz and the other, anonymous, reviewer(s) for their contribution to the peer review of this work. A peer review file is available.